

# **HHS Public Access**

Author manuscript

Annu Int Conf IEEE Eng Med Biol Soc. Author manuscript; available in PMC 2022 January 12.

Published in final edited form as:

*Annu Int Conf IEEE Eng Med Biol Soc.* 2021 November ; 2021: 6547–6550. doi:10.1109/EMBC46164.2021.9629884.

## Modeling ON Cone Bipolar Cells for Electrical Stimulation

## Javad Paknahad [Graduate Student Member, IEEE],

Department of Electrical Engineering, University of Southern California, Los Angeles, CA 90089 USA

## Pragya Kosta [Member, IEEE],

Institute for Technology and Medical Systems (ITEMS), Keck School of Medicine, University of Southern California, Los Angeles, CA 90089 USA.

## Ege Iseri,

Department of Biomedical Engineering, University of Southern California, Los Angeles, CA 90033 USA.

#### Shayan Farzad,

Department of Biomedical Engineering, University of Southern California, Los Angeles, CA 90033 USA.

#### Jean-Marie C. Bouteiller [Senior Member, IEEE],

Department of Biomedical Engineering, University of Southern California, Los Angeles, CA 90033 USA.

#### Mark S. Humayun [Fellow, IEEE],

Departments of Ophthalmology and Biomedical Engineering, University of Southern California, Los Angeles, CA 90033 USA.

## Gianluca Lazzi [Fellow, IEEE]

Departments of Electrical Engineering, Biomedical Engineering, and Ophthalmology, University of Southern California, Los Angeles, CA 90089 USA

## **Abstract**

Retinal prosthetic systems have been developed to help blind patients suffering from retinal degenerative diseases gain some useful form of vision. Various experimental and computational studies have been performed to test electrical stimulation strategies that can improve the performance of these devices. Detailed computational models of retinal neurons, such as retinal ganglion cells (RGCs) and bipolar cells (BCs), allow us to explore the mechanisms underlying the response of cells to electrical stimulation. While electrophysiological studies have shown the presence of voltage-gated ionic channels in different regions of BCs, many of the existing cone BCs models are assumed to be passive or only contain calcium channels at the synaptic terminals. We have utilized our Admittance Method (AM)-NEURON computational platform to implement a more realistic model of ON-BCs. Our model closely replicates the recent patch-clamp

J. Paknahad is with the Department of Electrical Engineering, University of Southern California, Los Angeles, CA 90089 USA, paknahad@usc.edu. G. Lazzi is with the Departments of Electrical Engineering, Biomedical Engineering, and Ophthalmology, University of Southern California, Los Angeles, CA 90089 USA, lazzi@usc.edu.

experiments directly measuring the response of ON-BCs to epiretinal electrical stimulation and thereby predicts the regional distributions of the ionic channels. Our computational results further indicate that outward potassium current strongly contributes to the depolarizing voltage transient of ON-BCs in response to electrical stimulation.

## I. Introduction

Retinal prosthetic systems help patients with retinal degenerative diseases, such as retinitis pigmentosa (RP) and aged-related macular degeneration (AMD), partially perceive objects, letters, and colors [1]–[6]. Retinal degeneration starts with the progressive loss of photoreceptors and further leads to remodeling and rewiring of the retinal circuitry [7]. Retinal implant-based prosthetic systems focus on the electrical stimulation of the surviving cells of degenerated retina to restore sight to the blind. Several prosthetic systems have been developed; however, the efficacy of these devices is still limited. One of the problems faced with epiretinal implants is the axonal activation of retinal ganglion cells (RGCs) which contributes to the elongated phosphene reported by the subjects, leading to the reduced spatial resolution of these devices [8]. In addition, activation threshold of RGCs has also been shown to be higher in degenerated retina [9], thereby requiring higher stimulation amplitudes which may lead to tissue damage. Therefore, it is essential to maximize the efficiency of the stimulation while reducing the stimulation threshold to avoid activation of RGCs axon bundles and potential tissue damage.

Many attempts have been conducted to enhance the efficacy of current epiretinal implants by directly and indirectly targeting RGCs [10]–[12]. Similarly, different electrical stimulation strategies have been proposed to enhance the efficacy of these devices and reduce the excitation threshold of RGCs [12], [13]. Several computational modeling approaches have been investigated to further understand the underlying mechanisms that result in varying sensitivity of retinal neurons to electrical stimulation. For example, the low stimulation threshold of the axon initial segment (AIS) of RGCs relative to the distal axon using short pulse durations has been shown to be effective in achieving more focal response of RGCs [12].

In addition to comprehensive development of RGCs models, there have been electrophysiological studies focusing on identifying the expression of voltage-gated ionic channels in BCs [14], [15]. A detailed model of spiking BCs in the magnocellular pathway of the primate retina, diffuse bipolar cells (DB4), has been implemented by *Rattay et al.* [16], [17]. Although the presence of active membrane properties has been shown in both ON and OFF BCs, the other available BC models were either assumed to be passive or only expressed L-type and T-type calcium channels at the presynaptic terminals of the cells [18]–[22]. In a few studies, the reported impact of potassium reversal potential on the calcium reversal potential of BCs has been incorporated into the model of BCs [19], [20]. The role of other regional voltage-gated ionic channels in shaping the BCs response to external stimulation was assumed to be negligible [19]. However, no experiment was performed to investigate the sensitivity of BCs response to variations in densities and distributions of ionic channels to support this assumption.

Recently, a novel photoreceptor peeling technique has been developed to directly record the ON-type mouse BCs response to epiretinal electrical stimulation [23]. The depolarizing voltage transients have been measured at the cell bodies of the ON-BCs [24]. In this study, we have utilized the multi-scale Admittance Method (AM)-NEURON computational platform [6], [9], [25]–[27], integrating the recent experimentally recorded signals of BCs, to predict the expressions and distributions of ionic channels in each cellular region of the cell. The biophysically detailed and realistic model of ON-BCs would allow us to better capture the mechanisms underlying their response to electrical stimulation. The implemented model was able to closely reproduce the response of ON-BCs measured experimentally to epiretinal electrical stimulation [24]. The model also suggests the contribution of the outward potassium current, along with the L-type calcium channel, to the depolarizing transient response of BCs to epiretinal electrical stimulation.

#### II. Methods

#### A. **NEURON Simulation**

The change in cell membrane potential in response to an applied external stimulation is computed using NEURON computational software [28]. The cell is modeled in a multi-compartmental approach, where the soma, axon, terminals, and dendrites are defined as separate compartments (Fig. 1). The morphology of the cell is extracted as an SWC file from the previous work [17]. Each cell branch has unique biophysical properties that are expressed as passive or active ionic membrane channels. Therefore, the mechanism of current flow and potential generation varies across the cell depending on the channel distributions at various cell regions. n. The membrane conductance values, and distributions of ionic channels are represented in Fig. 1. Most of the voltage-dependent rate constants and ionic kinetics can be found in [17]. The L-type Ca channel has been adjusted from the previous work and its kinetics are governed by [19]:

$$i_{CaL} = g_{CaL} c^3 (V - E_{caL}) \tag{1}$$

$$\frac{dc}{dt} = -(\alpha_c + \beta_c)c + \alpha_c \tag{2}$$

$$\alpha_c = \frac{-0.3(V+70)}{e^{-0.1}(V+70)_{-1}} \tag{3}$$

$$\beta_C = 10 e^{-(V + 38)/9}$$

Where  $g_{CaL}$  is the maximum membrane conductance of the L-type calcium and the activation gating variable is c. The rate constants  $\alpha$  and  $\beta$  represent opening and closing of the channels. The reversal potential of the calcium channel ( $E_{CaL}$ ) is formulated based on the intracellular concentration of the calcium, according to *Fohlmeister et al.* [29]. The extracellular calcium concentration is set to 1.8 mM. The depth of the calcium pump and

the time constant of the calcium current are  $0.1~\mu m$  and 1.5~ms, respectively. The membrane capacitance and intracellular resistivity are set to  $3~\mu F/cm^2$  and  $100~\Omega$ .cm. The resting membrane voltage is -55~mV, and the reversal potential of the potassium is adjusted to -90~mV to better replicate the experimental recorded signals, including the peak and resting membrane potentials. Further details of the remaining parameters and variables can be found in [17].

#### **B.** AM-NEURON Computational Platform

The NEURON simulations are combined with the AM to obtain cell response to an external electrical stimulation. This multi-scale simulation framework simulates a 3D bulk tissue model and the neuronal model as shown in Fig. 1. The stimulating electrode and various retina layers with respective resistivity properties are implemented in the bulk tissue model. The AM discretizes the bulk tissue model and computes the voltage induced due to electrical stimulation at every node of computational cells. These computed voltage values are then interpolated at the center of each compartment of the neuron model. Finally, neuronal response is simulated by applying the interpolated voltages as the extracellular voltage at every compartment. Further details about the modeling approach, including the properties of the retinal layers, can be found in [9], [26], [27], [28]. Using this method, we can predict how cells might respond to stimulation waveforms generated by an implanted electrode in the 3-D space.

## III. Results

## A. Verification of the model with Experiments

The ionic channels distributions and densities in each region of the multi-compartment model of the ON-BCs have been selected to closely predict the behavior of the cells to epiretinal electrical stimulation. Fig. 2 shows the membrane voltage recorded from the soma in response to epiretinal electrical stimulation for both the implemented model and experimental measurements provided by Walston et al. [24]. The symmetric cathodic-first charge-balanced biphasic pulses are applied and the response of the cell is compared for pulse widths (PW) of 8 ms and 25 ms. The BCs model closely predicts the response characteristics of the cell to electrical stimulation of varying pulse widths and amplitudes. At the onset of the cathodic phase, the membrane potential at the soma hyperpolarizes due to the longer distance of the stimulating electrode from the cell body relative to the terminals [16]. The depolarized signals from the terminal of the cell backpropagate towards the soma, thereby leading to the depolarization of the cell following the hyperpolarization (Fig. 2). The strong depolarizing voltage response occurs after the termination of the cathodic stimulation (the onset of the anodic stimulation). An increase in the current amplitude slightly increases the maximum negative potential at the onset of the cathodic phase (Fig. 2). A stronger current stimulus is shown to reduce the duration of the negative potential. This may arise from the delayed opening of the voltage-gated ionic channels at the threshold compared to high suprathreshold current amplitudes.

## B. Sensitivity of BCs Response to Na channel

We investigated the contribution of each active ionic current to the response properties of the ON-BCs. We further considered the sensitivity of the BCs response to the presence of sodium (Na) current concentrated in the axon of spiking BCs. For a given current amplitude, the duration of the hyperpolarized potential is reduced in the presence of the Na current as shown in Fig. 3a. Due to the opening of the Na channel, the delayed response of the peak membrane potential during the cathodic phase has been decreased. The addition of the Na current decreases the stimulation threshold of BCs (Fig. 3a). The ionic currents of each section are represented in Fig. 3b. The strong outward potassium currents in the axon and soma of the cell are predicted from the BCs model, which contribute to the peak depolarization of membrane after the termination of the cathodic pulse stimulation. This is in agreement with the results of recent voltage-clamp experiments on the ON-type mouse BCs, suggesting the presence of a strong outward rectifying potassium current in this cell type [23].

## C. Blockage of L-type Ca channel

We examined the role of the L-type Ca channel in the response of ON-BCs to electrical stimulation. Interestingly, the removal of the L-type Ca channel eliminated the depolarizing voltage transients of the cell at the onset of the cathodic phase as shown in Fig. 4. Further increase in the strength of the electrical stimulation to  $120~\mu A$  for a given pulse duration of 8 ms did not result in the opening of the voltage-gated ionic channels. This indicates the significant contribution of the calcium channels concentrated at the synaptic terminals of BCs to the active response of cells to electrical stimulation. The depolarizing voltage transients are originated in the terminals of the cell and mediated by the L-type Ca channels (Fig. 4). This correlates well with the recent experimental data suggesting the addition of the cadmium chloride (Cdcl<sub>2</sub>), pharmacological blocker of the calcium current, eliminates the depolarizing voltage transient response of ON-BCs to epiretinal electrical stimulation [24].

## IV. Discussion and Conclusion

We have utilized our 3D combined AM-NEURON computational platform to estimate the distribution and density of voltage-gated ionic channels in ON-BCs. Research has been conducted in developing biophysical properties of cells in response to intracellular stimulation and predicting the expression and kinetics of each ion in isolation [16]–[20]. However, extracellular stimulation may allow us to better determine the distribution of ions and their roles in forming the response to electrical stimulation. Using this modeling framework, we developed the ON-BCs model incorporating more realistic channel allocations compared to the existing models [18]–[21]. We verified the ON-BCs biophysical model by testing our simulations against comparable experimental recordings. Compared to previous works, our model contains potassium channels at the soma, axon, and dendrites of the cell. The presence of the Na channel in the axon and its role in the response pattern and stimulation threshold of the cell to electrical stimulation were investigated. The model further shows that the blockage of the L-type Ca current can suppress the active response of ON-BCs to electrical stimulation.

Notably, there is a discrepancy in the current amplitude of computational modeling and experiment results (Fig. 2). The significant differences in the resistivity of the retina reported in the literature [17], [25], and the potential dissimilarity in electrode-to-cell distance position in whole cell patch-clamp experiments compared to the modeling approach may contribute to the current threshold difference. In this study, we mostly aimed at determining the distributions of ionic channels for a given morphology to replicate the biophysical response of the bipolar cells. However, morphological factors such as the length of the axon and intracellular properties can play important roles is shaping the response of cells [18]. In the future, we will incorporate morphologically different subtypes of BCs and investigate their response to a range of electrical stimulation parameters. This sensitivity analysis of morphologically and biophysically detailed models of BCs would help shed some light on the mechanisms underlying the hypersensitivity of BCs to long stimulus pulses or low sinusoidal stimulation frequencies reported in the literature [10], [18]. Finally, the present study illustrates the effectiveness of the multiscale computational platform in replicating realistic cell models and predicting their response to electrical stimulation, thereby guiding the design of efficient stimulation strategies.

## **Acknowledgment**

We would like to thank the authors of Walston et al. (2018) for sharing their BCs patch clamp experimental data that bolstered the development of our BC model and comparing the simulated response with the experimental recordings.

This work was supported by the EFRI NSF (Award No. 1933394), NEI (NIH Grant No. R21EY028744), the NIBIB (NIH Grant No. U01EB025830), and an unrestricted grant to the Department of Ophthalmology from Research to Prevent Blindness, New York, NY.

## References

- [1]. Humayun MS et al., "Visual perception in a blind subject with a chronic microelectronic retinal prosthesis," Vision Res, vol. 43, no. 24, pp. 2573–2581, 2003. [PubMed: 13129543]
- [2]. Weiland JD and Humayun MS, "Retinal Prosthesis," Tbme, vol. 61, no. 5, pp. 1412-1424, 2014.
- [3]. Stingl K et al., "Subretinal Visual Implant Alpha IMS Clinical trial interim report," Vision Res, vol. 111, pp. 149–160, 2015. [PubMed: 25812924]
- [4]. Ahuja AK and Behrend MR, "The Argus<sup>™</sup> II retinal prosthesis: Factors affecting patient selection for implantation," Prog. Retin. Eye Res, vol. 36, pp. 1–23, 2013. DOI: 10.1016/j.preteyeres.2013.01.002. [PubMed: 23500412]
- [5]. Kosta P, Paknahad J, Rodriguez ESG, Loizos K, Roy A, Talbot N, Seidman S, Datta P, Dai R, Pollack B, Greenberg R, and Lazzi G, "Electromagnetic Safety Assessment of a Cortical Implant for Vision Restoration," IEEE Journal of Electromagnetics, RF and Microwaves in Medicine and Biology, vol. 2, no. 1, pp. 56–63, 2018.
- [6]. Paknahad J, Loizos K, Yue L, Humayun MS, and Lazzi G, "Color and cellular selectivity of retinal ganglion cell subtypes through frequency modulation of electrical stimulation," Scientific Reports; Sci Rep, vol. 11, no. 1, pp. 5177, 2021. [PubMed: 33664347]
- [7]. Jones BW et al., "Retinal remodeling in the Tg P347L rabbit, a large-eye model of retinal degeneration," J. Comp. Neurol, vol. 519, no. 14, pp. 2713–33, 2011. [PubMed: 21681749]
- [8]. Beyeler M et al., "A model of ganglion axon pathways accounts for percepts elicited by retinal implants," Scientific Reports, vol. 9, no. 1, pp. 9199, 2019. [PubMed: 31235711]
- [9]. Loizos K, Marc R, Humayun MS, Anderson JR, Jones BW, and Lazzi G, "Increasing Electrical Stimulation Efficacy in Degenerated Retina: Stimulus Waveform Design in a Multiscale Computational Model," IEEE Transactions on Neural Systems and Rehabilitation Engineering, vol. 26, no. 6, pp. 1111–1120, 2018. [PubMed: 29877835]

[10]. Weitz AC et al., "Improving the spatial resolution of epiretinal implants by increasing stimulus pulse duration," Science Translational Medicine, vol. 7, no. 318, pp. 318ra203, 2015.

- [11]. Jensen RJ, Ziv OR, and Rizzo JF, "Thresholds for Activation of Rabbit Retinal Ganglion Cells with Relatively Large, Extracellular Microelectrodes," Invest. Ophthalmol. Vis. Sci, vol. 46, no. 4, pp. 1486, 2005. DOI: 10.1167/iovs.04-1018. [PubMed: 15790920]
- [12]. Paknahad J, Loizos K, Humayun MS, and Lazzi G, "Targeted Stimulation of Retinal Ganglion Cells in Epiretinal Prostheses: A Multiscale Computational Study," Theore, vol. 28, no. 11, pp. 2548–2556, 2020. DOI: 10.1109/TNSRE.2020.3027560.
- [13]. Hadjinicolaou AE et al., "Optimizing the electrical stimulation of retinal ganglion cells," IEEE Transactions on Neural Systems and Rehabilitation Engineering, vol. 23, no. 2, pp. 169–178, 2015. [PubMed: 25343761]
- [14]. Puthussery T et al., "NaV1.1 Channels in Axon Initial Segments of Bipolar Cells Augment Input to Magnocellular Visual Pathways in the Primate Retina," Journal of Neuroscience, vol. 33, no. 41, pp. 16045–16059, 2013. [PubMed: 24107939]
- [15]. Benav H, "Modelling effects of extracellular stimulation on retinal bipolar cells." (Ph.D. thesis). Eberhard-Karls-Universitaet Tuebingen, 2012.
- [16]. Rattay F, Bassereh H, and Fellner A, "Impact of Electrode Position on the Elicitation of Sodium Spikes in Retinal Bipolar Cells," Scientific Reports, vol. 7, no. 1, pp. 17590, 2017. [PubMed: 29242502]
- [17]. Rattay F, Bassereh H, and Stiennon I, "Compartment models for the electrical stimulation of retinal bipolar cells," PloS One, vol. 13, no. 12, pp. e0209123, 2018. [PubMed: 30557410]
- [18]. Freeman DK et al., "Calcium channel dynamics limit synaptic release in response to prosthetic stimulation with sinusoidal waveforms," Journal of Neural Engineering; J Neural Eng, vol. 8, no. 4, pp. 046005, 2011.
- [19]. Werginz P and Rattay F, "The impact of calcium current reversal on neurotransmitter release in the electrically stimulated retina," Jne, vol. 13, no. 4, pp. 046013, 2016. [PubMed: 27296730]
- [20]. Werginz P et al., "Modeling the response of ON and OFF retinal bipolar cells during electric stimulation," Vision Res, vol. 111, pp. 170–181, 2015. [PubMed: 25499837]
- [21]. Publio R, Oliveira RF and Roque AC, "A computational study on the role of gap junctions and rod Ih conductance in the enhancement of the dynamic range of the retina," PloS One, vol. 4, (9), pp. e6970, 2009. [PubMed: 19777063]
- [22]. Kosta P, Iseri E, K Loizos, Paknahad J, Pfeiffer RL, Sigulinsky CL, Anderson JR, Jones BW, and Lazzi G, "Model-based comparison of current flow in rod bipolar cells of healthy and early-stage degenerated retina," Exp. Eye Res, pp. 108554, 2021. [PubMed: 33794197]
- [23]. Walston ST et al., "Method to remove photoreceptors from whole mount retina in vitro," J. Neurophysiol, vol. 118, no. 5, pp. 2763–2769, 2017. [PubMed: 28855296]
- [24]. Walston ST, Chow RH and Weiland JD, "Direct measurement of bipolar cell responses to electrical stimulation in wholemount mouse retina," Jne, vol. 15, no. 4, pp. 046003, 2018. [PubMed: 29513646]
- [25]. Loizos K, Ramrakhyani AK, Anderson J, Marc R, and Lazzi G, "On the computation of a retina resistivity profile for applications in multi-scale modeling of electrical stimulation and absorption," Phys. Med. Biol, vol. 61, no. 12, pp. 4491–4505, 2016. DOI: 10.1088/0031-9155/61/12/4491. [PubMed: 27223656]
- [26]. Stang J et al., "Recent Advances in Computational and Experimental Bioelectromagnetics for Neuroprosthetics," Iceaa, pp. 1382, 2019. DOI: 10.1109/ICEAA.2019.8878960.
- [27]. Paknahad J, Loizos K, Humayun MS, and Lazzi G, "Responsiveness of retinal ganglion cells through frequency modulation of electrical stimulation: A computational modeling study\*," in 2020 42nd Annual International Conference of the IEEE Engineering in Medicine & Biology Society (EMBC), 2020.
- [28]. Hines ML and Carnevale NT, "The NEURON simulation environment," Neural Computation, vol. 9, pp. 1179–1209, 1997. [PubMed: 9248061]
- [29]. Fohlmeister JF and Miller RF, "Impulse encoding mechanisms of ganglion cells in the tiger salamander retina," J. Neurophysiol, vol. 78, no. 4, pp. 1935–1947, 1997. [PubMed: 9325362]

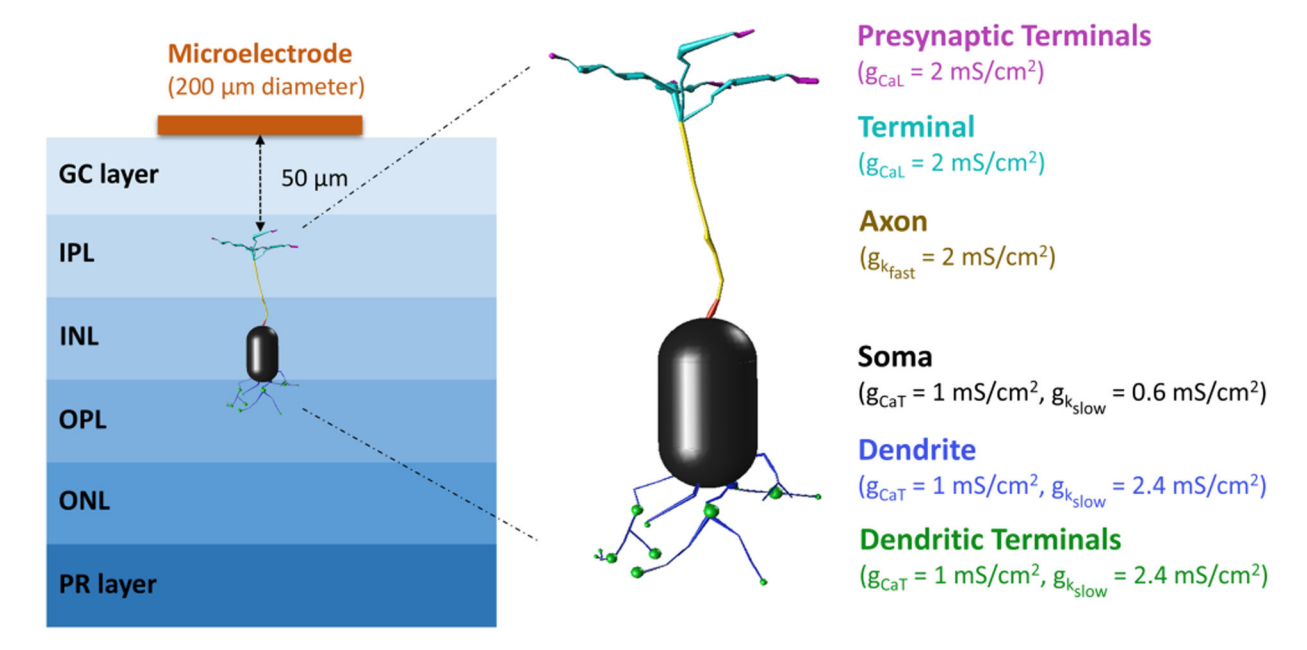


Fig. 1. Multi-scale model consisting of (a) bulk tissue model with microelectrode, various retinal layers (GC: ganglion cell; IPL: inner plexiform layer; INL: inner nuclear layer; OPL: outer plexiform layer; ONL: outer nuclear layer; PR: photoreceptor) and (b) morphologically detailed retinal bipolar cell model. The stimulating electrode of 200  $\mu$ m diameter is placed 50  $\mu$ m from the synaptic terminals of BCs. The bulk retinal tissue model is utilized to compute the voltages at every node of the model due to the stimulating microelectrode. These extracellular voltages are then applied to the bipolar cell model to simulate its spatio-temporal response to electrical stimulation.

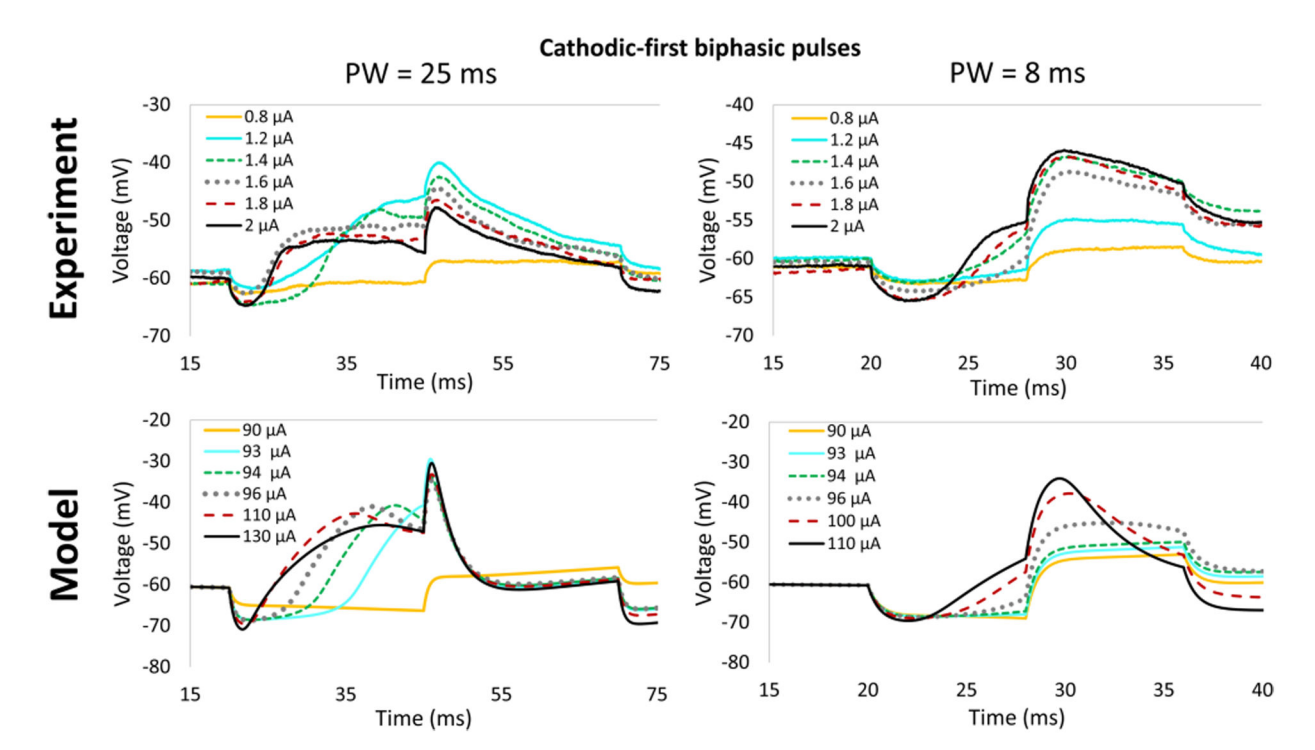


Fig. 2. The response of the ON-type BCs to epiretinal electrical stimulation of various pulse amplitudes using symmetric biphasic cathodic-first charge-balanced stimulus pulses of 8 ms and 25 ms durations. Top figures: experimental recording signals from [24]. Bottom figures: modeling results using AM-NEURON platform. Results indicate that the model can closely predict the experimentally recorded response characteristics of ON-BCs to epiretinal electrical stimulation.

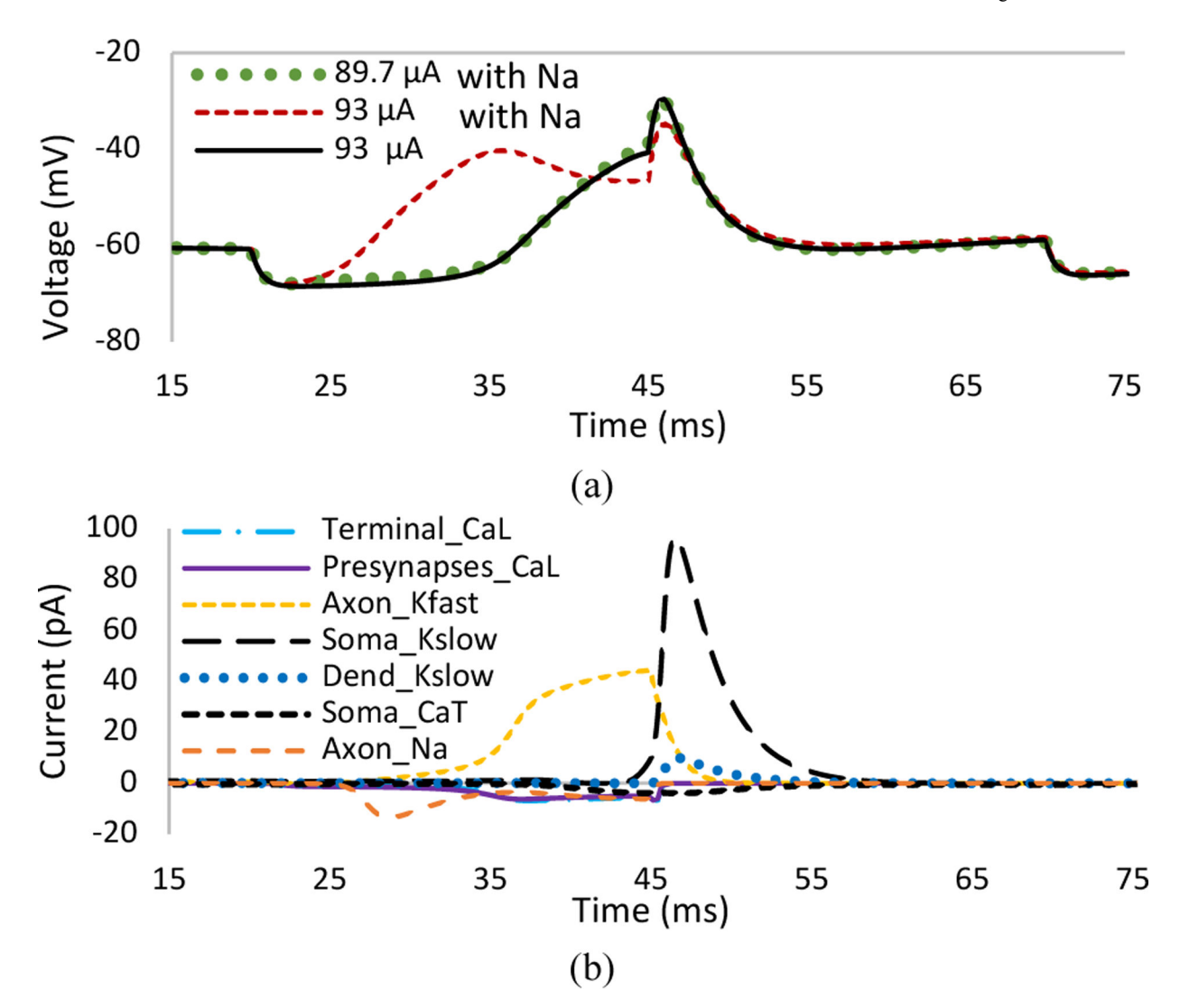


Fig. 3. (a) The transmembrane potential elicited by the extracellular stimulation of a symmetric cathodic-first biphasic pulse of 25 ms in the presence and absence of the Na channel. (b) The ionic currents in different regions of the cell at 93  $\mu$ A stimulus amplitude. The membrane conductance value of the Na channel in the axon is set to 300 mS/cm<sup>2</sup>.

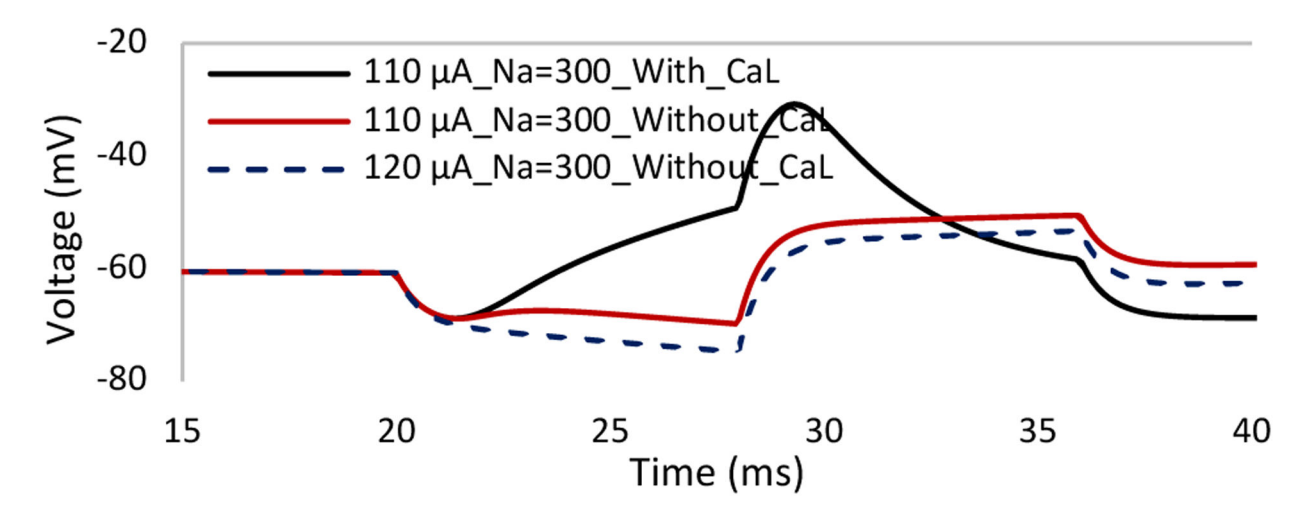


Fig. 4. The role of L-type calcium channel at the terminal of BCs in the depolarizing voltage transients at the onset of the cathodic stimulation pulse. The stimulus pulse duration is set to 8 ms. Data show that the active response properties of the cell is eliminated in the absence of the L-type channel, even at higher current amplitude of  $120~\mu A$ .